Floodplain Conservation Versus Landscape Development—How to Tackle the Multifunctional Management Issue

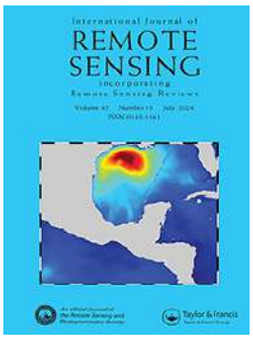

International Journal of Remote Sensing

ISSN: (Print) (Online) Journal homepage: www.tandfonline.com/journals/tres20

Enhancing precision in coastal dunes vegetation mapping: ultra-high resolution hierarchical classification at the individual plant level

E. Belcore, M. Latella, M. Piras & C. Camporeale

To cite this article: E. Belcore, M. Latella, M. Piras & C. Camporeale (2024) Enhancing precision in coastal dunes vegetation mapping: ultra-high resolution hierarchical classification at the individual plant level, International Journal of Remote Sensing, 45:13, 4527-4552, DOI: 10.1080/01431161.2024.2354135

To link to this article: https://doi.org/10.1080/01431161.2024.2354135

Published online: 26 Jun 2024.

INTERNATIONAL JOURNAL OF REMOTE SENSING
2024, VOL. 45, NO. 13, 4527–4552
https://doi.org/10.1080/01431161.2024.2354135

Taylor & Francis
Taylor & Francis Group

Enhancing precision in coastal dunes vegetation mapping: ultra-high resolution hierarchical classification at the individual plant level

E. Belcore [a], M. Latella [b], M. Piras [a] and C. Camporeale [a]

[a]Department of Environment, Land and Infrastructure Engineering (DIATI), Politecnico di Torino, Torino, Italy; [b]CMCC Foundation – Euro-Mediterranean Center on Climate Change, Viterbo, Italy

ABSTRACT

The classification of ultra-high-resolution (UHR) imagery, characterized by spatial resolutions exceeding 10 cm, presents opportunities and challenges distinct from lower-resolution counterparts. Particularly, challenges are pronounced in some scenarios, such as mapping plant species in coastal environments, where similar vegetation responses and small plant sizes pose additional difficulties. The present work addressed such issues by developing a UHR vegetation cover classification model at the single plant level using data from uncrewed aerial systems (UASs) equipped with a multispectral optical sensor. The model was tested across the San Rossore Regional Park (Italy), where three pilot areas were defined as training-test-validation sites. The proposed solution consists of a hierarchical two-level-of-detail machine learning model based on object-based image analysis (OBIA) and random forest. This model considers spectral features and indices, elevation, and texture and can classify twelve plant species and two service classes (debris and sand) within the study areas. Train and test were carried out utilizing UAS flight data collected during two specific phenological periods and precise field data derived from in-situ vegetation surveys, which provided 937 herbaceous and shrub samples. The model performance was evaluated based on the error matrix and 50-fold stratified cross-validation method, obtaining an overall accuracy (OA) of 0.76 and a standard deviation of 0.08. Such assessment underscored the crucial role of texture information, in addition to radiometric and elevation. Finally, the model was tested against an unseen dataset, proving its transferability (OA equal to 0.62). Although the discussion highlights some aspects to be further improved and claims for future research, the first version of this hierarchical classification model demonstrated its potential for mapping and monitoring coastal sand dune ecosystems, providing data for understanding and, eventually, modeling ecological and biogeomorphological dynamics.

ARTICLE HISTORY
Received 31 January 2024
Accepted 26 April 2024

KEYWORDS
Coastal vegetation mapping; ultra-high-resolution (UHR); Unmanned Aerial Systems (UAS)

CONTACT M. Latella melissa.latella@cmcc.it CMCC Foundation – Euro-Mediterranean Center on Climate Change, Via Igino Garbini 51, Viterbo 01100, Italy

1. Introduction

Earth's surface is commonly described through land cover (LC), which provides information about biotic and abiotic assemblages in a specific area (Townshend 1992; Wulder et al. 2018). The knowledge of its change in time is pivotal for environmental sciences, land and urban planning, and natural resource management from local up to national and regional scales (Turner, Eric, and Reenberg 2007; Verburg et al. 2019).

Remote sensing (RS) supports mapping and monitoring LC in a relatively simple and fast way compared to traditional field surveys (Herold et al. 2006; Wulder et al. 2018). The first RS-based LC classifications used to rely on visual interpretation of orthomosaics of three spectral bands only (R, G, B). However, nowadays, multispectral and hyperspectral imagery allows for performing high-accuracy classifications in several contexts, especially when leveraging specific combinations of spectral bands to compute radiometric indices, like the widely-used Normalized Difference Vegetation Index (NDVI), that support detecting land cover changes (Campos-Taberner et al. 2023; Gromny et al. 2022) and determining soil and vegetation status (Babaeian et al. 2021; Horning et al. 2020).

Multispectral sensors can be mounted across different vectors (tripods, drones, aircraft, or satellites), each providing information with diverse time and spatial resolution. Among these, drones, also referred to as Uncrewed Aerial Systems (UAS) and Uncrewed Aerial Vehicles (UAV), have gained approval for research in recent years, allowing to perform meaningful analysis in a wide range of scientific fields, ranging from disaster monitoring (Calantropio et al. 2018), forestry (Fawcett, Bennie, and Anderson 2021; N. Zhang et al. 2023), freshwater sciences (Piégay et al. 2020; Wawrzyniak et al. 2013; Woodget et al. 2017), ecology (Belloni et al. 2023; Cortesi et al. 2022; Ioli et al. 2020; Lou et al. 2023) and civil engineering (Patrucco et al. 2022; Zollini et al. 2020), among others. Moreover, the spread of drones has paved the way for new horizons of LC classification and, as (Horning 2020) points out, the interest in LC classification from high-resolution optical data acquired by aerial drone systems has markedly increased in the last few years. The cost-effectiveness and low time consumption of UAS, especially if compared to traditional mapping methods like field surveys and aerial photos from aircraft, facilitate multi-temporal studies and monitoring activities (Belcore et al. 2022; Schiefer et al. 2020). In addition, sensors mounted on UAS often enable ultra-high-resolution (UHR) LC classification, which means spatial resolutions finer than 0.1 m, in contrast with the very-high-resolution (VHR) offered by the sensors more frequently mounted on other vectors (i.e. spatial resolutions lower than 1.0 m).

Although employing UAS systems for UHR LC classifications is widespread, most of the works concerning natural environments rely on classifying plant species instead of LC (Agrillo et al. 2022; Ahmed et al. 2017; Bhatt and Maclean 2023; Cruz et al. 2023; Horning et al. 2020; Kattenborn et al. 2020; Michez et al. 2016; Schiefer et al. 2020). In this sense, coastal dunes are a notable example of a dual necessity of both LC and plant-feature mapping.

The coastal dune ecotone hosts transitional habitats between aquatic and terrestrial ecosystems, therefore playing a fundamental role in the functional biotic and abiotic connectivity (Acosta, Blasi, and Stanisci 2009; Carboni, Laura Carranza, and Acosta 2009). This transition generates gradients of environmental disturbances (e.g. wind, waves, salt spray, sand movement, groundwater depth) and physical parameters (e.g. soil moisture

and salinity), inducing an ecological succession of plant species called *psammosere* (Ritchie 1972) and representing an ecological corridor for fauna (Kutiel 2001). Because of the high biodiversity of coastal dunes, high-resolution vegetation mapping and species recognition are necessary to analyze biological dynamics and plant patterns. On the other hand, LC classification supports investigating the interaction between vegetation and the surrounding environment (Suo, McGovern, and Gilmer 2019), providing useful information for coastal management, conservation, and restoration.

Despite its usefulness, UHR LC classification of coastal dune ecosystems is intricate, primarily due to: i) the extreme similarity of vegetation spectral responses to multispectral sensors (Horning et al. 2020); ii) the size and features of vegetation, which is predominantly herbaceous or constituted by small plants (approximately 0.05 m^2 cover) with low density and alternating with other elements of varying spectral response (sand, rocks, woody debris, spastic debris, algal and shell deposits, water); and iii) the influence of climate on vegetation, causing dune plants to appear dry or leafless for much of the summer period in the Mediterranean region or inducing their shrinking during the dormant winter season in cold regions, Maun (2020).

The literature suggests several techniques to classify land cover from UHR data accurately, and these can also be translated and applied in natural environments such as dune ecosystems. Among these, we underscore four of the most promising solutions, to the best of our knowledge, in the following.

The first one is the classification at hierarchical levels of detail, which we will henceforth refer to as Level of Detail (LoD). LoD methodologies are rapidly catching on (Ahmed et al. 2017; Laporte-Fauret et al. 2020). They generally perform an initial classification with low thematic detail (first hierarchy level) and subsequently focus on high thematic resolution classifications of one (or more) 1-level classes. Such an approach has already been consolidated in satellite LC classifications. For instance, the Food and Agriculture Organization (FAO) adopts a hierarchical and multi-level approach in its Land Cover Classification System (LCCS) (Di Gregorio and Food and Agriculture Organization of the United Nations 2005).

A second strategy to address UHR LC classification of coastal dunes is adopting a multitemporal approach. Similar to the case of LoD, this kind of solution is consolidated for satellites but rarely applied to drone datasets, likely because of the more significant resources required to perform two or more UAS acquisitions (Michez et al. 2016; Shi et al. 2020). However, some authors have started exploring the UHR multitemporal approach by including plant phenology in the classification as an intrinsic variable (Belcore et al. 2021; Michez et al. 2016; Shi et al. 2020; Takahashi Miyoshi et al. 2020), achieving promising results.

The third solution is the use of textural information in the classification. It must be noted that this approach is generally well-established for UHR-UAS data but not in coastal environments (Agrillo et al. 2022; Bhatt and Maclean 2023; Horning et al. 2020; Lou et al. 2023).

Finally, to address intra-class variability and low spectral separability, the literature suggests using the object-based image analysis (OBIA) method (Lou et al. 2023; Melville, Fisher, and Lucieer 2019; X. Zhang et al. 2017). Indeed, OBIA improves class separability by considering additional features such as spatial, texture, and contextual information (Kalantar et al. 2017). A well-known application is represented by OBIA-LC classifications of urban or generally artificial areas (Belcore, Piras, and Pezzoli 2022; Park et al. 2022; Trevisiol et al. 2022;

Wyard et al. 2022), where concrete roofs and parking lots have a very similar spectral signature but different texture and shape (Kuras et al. 2021). It is worth noting that another option can be using deep learning, whose applications for mapping and performing remote sensing tasks are spreading, proving accuracy and preciseness. However, when moving to complex environments, such as natural forests, instance segmentation (separating different trees or plants and classifying them) is still difficult. Deep learning algorithms are able to perform on many classes if properly trained on large datasets, yet this kind of datasets is difficult to construct. Some studies address this challenge by facing instance segmentation in two steps, namely (i) using the traditional OBIA approach to segment vegetation and (ii) deep learning for species classification (Diez et al. 2021).

We remark that when a UHR OBIA LC classification is applied to vegetated areas, the objects, or segments, of the classification are represented by plants grouped into communities or plant functional types (PFTs) (Agrillo et al. 2022; Räsänen et al. 2019; Sankey et al. 2021). PFTs have significance at an ecological and botanical level but little in terms of spectral response. Indeed, even if PFTs hold great importance in (coastal) ecology studies, they can be misleading when applied at the OBIA land cover level, where areas with dissimilar spectral characteristics are segmented. Due to the averaging of spectral and textural responses of pixels within a specific cover class, the PFTs approach applied to UHR data can result in an approximation that jeopardizes the transferability of classification models to different areas. These aspects are difficult to assess because model transferability remains one of the least tested features in most classification works.

In agreement with previous works (Natesan, Armenakis, and Vepakomma 2020; Prošek and Šímová 2019; Schiefer et al. 2020; Shi et al. 2020; Sothe et al. 2019; Suo, McGovern, and Gilmer 2019), we argue that in natural ecosystems, especially where vegetation is not dense, a multi-level classification based on OBIA is needed. In this sense, a first level should comprise a high-resolution LC map, while further levels can provide plant-specific information necessary to address ecological dynamics.

Given the ecological significance of coastal dune ecosystems, along with the challenges encountered in their vegetation mapping and the proposed solutions, this study seeks to construct a two-level object-based image analysis (OBIA) classification model. The first level involves semantic segmentation of vegetation cover, providing a single-plant detection, while the second level details the classification of plant species (Figure 1). This model also includes texture and multitemporal information to increase the robustness of classification. In the following, we describe the study site, comprising three pilot areas in the Migliarino-San Rossore-Massaciuccoli Regional Park (Italy), data collection and processing, and the setup of the classification algorithm. Subsequently, we report the results deriving from the model's application and the validation of the methodology. Finally, we comment on the most important results, opening up for discussion about further improvement of the presented approach and its potential application in the environmental sciences.

2. Material and methods

2.1. Study site

This work focuses on three pilot sites along the Tyrrhenian coastline in central Italy. These sites are part of the 23,000-ha protected areas of the Migliarino-San Rossore-Massaciuccoli

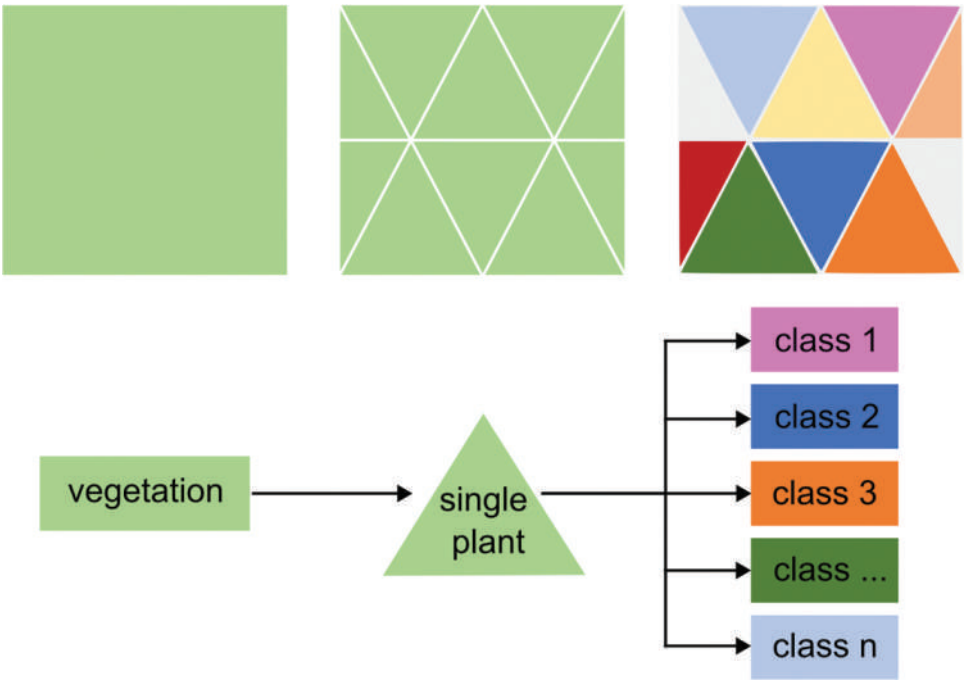

Figure 1. Simplified scheme of the adopted LC LoD classification. Level of detail 1 (LoD 1) consists of a single plant definition, while LoD2 assigns a class (i.e. species) to the identified segments.

Regional Park (Figure 2), established in 1979. This area was designated a Biosphere Reserve by UNESCO in 2004. Due to its ecological value and high biodiversity, this park has been the object of several studies (Barducci et al. 2007, 2009; Bertacchi 2017; Bertoni et al. 2014; Ciccarelli 2014; Ciccarelli, Garbari, and Bedini 2009; Cipriani et al. 2010; Fanini et al. 2007; Gellini et al. 1983; Mo et al. 2021; Scopetani et al. 2021).

We defined the three pilots as rectangular areas stretching approximately 500 m along the coastlines and 400 m transversally (area 1: 430 × 430 m; area 2: 500 × 370 m; area 3: 670 × 420 m). Altogether, the study sites cover 1.6 km of coastlines, representing 5.3% of the coastal sector of the park (Bertacchi 2017). The pilots extend across different vegetation patterns from the shoreline up to coastal dunes, retro-dunal areas, and xerophyte forests, embracing plant species from all the stages of the psammosere. The beach and dunes consist of calcareous sand and herbaceous vegetation comprising pioneers (*Achillea maritima* L., *Dittrichia viscosa* L., *Echinophora spinosa* L., *Eryngium maritimum* L., *Euphorbia paralias* L., *Helichrysum stoechas* L., *Pancratium maritimum* L.), dune-building grasses (*Ammophila arenaria* L.,) and evergreen shrubs (*Daphne Gnidium* L., *Juniperus oxycedrus macrocarpa* L., *Pinus Pinaster* Ait., *Pistacia lentiscus* L., *Yucca gloriosa* L.).

Area 1 is located at the Lecciona beach (43°49′51′N, 10°15′11′E), where no foredunes are present but a wide area of small shadow dunes covered by herbaceous plants and regularly distributed clusters of evergreen shrubs. The vegetation does not seem to suffer from human presence, which is intense throughout the year for beach tourism and sea sports. In contrast, we observed well-developed foredunes in Areas 2 and 3. Area 2 is located southward of the mouth of the Serchio River (43°46′05′N, 10°16′23′E), while Area 3

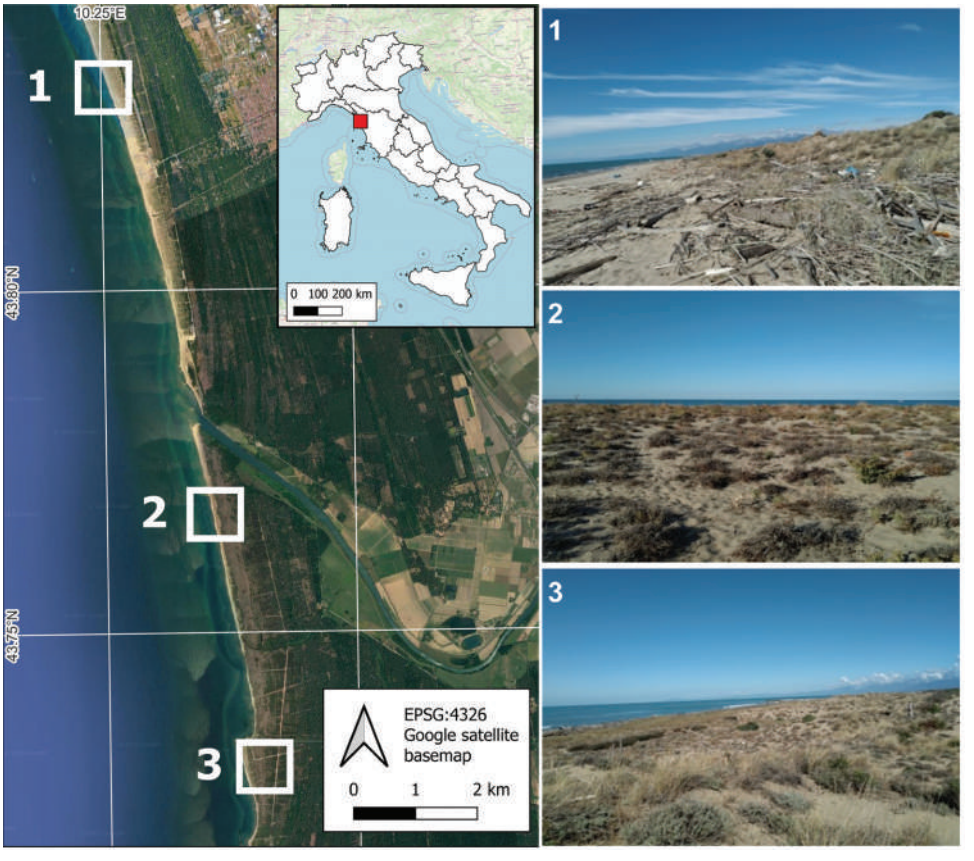

Figure 2. Localization of the Migliarino-San Rossore-Massaciuccoli Regional Park and the three pilot areas.

is southward of the mouth of the artificial channel called Fiume Morto Nuovo (43°43'48'N, 10°16'41'E). Direct human disturbance is low in these areas, yet the pervasive presence of marine litter blended with large woody debris threatens the ecosystems. Woody and litter debris are transported by relatively short-range longshore currents flowing from rivers' mouths (Mo et al. 2021) and long-range marine currents moving debris from Ligurian coasts.

2.2. Data collection and photogrammetric processing

We carried out a standard drone survey using multi-rotor uncrewed aerial systems (UASs) equipped with a multispectral optical sensor. We conducted two campaigns, choosing their timing according to phenological phases. The first data collection campaign, hereafter labeled *Autumn*, took place in September 2021, and the second, *Spring*, took place in May 2022 during the vegetation's maximum lush phase. We used a commercial multi-rotor UAS solution, *DJI Phantom 4 (P4) multispectral*. This UAS was embedded with five multispectral optics (Red, Green, Blue, Red edge, and NIR), a regular RGB sensor (Table 1), and a GNSS dual-frequency receiver.

Table 1. Characteristics of DJI phantom 4 multispectral embedded sensors; n.a. means not available.

Commercial name	Sensor	Focal length (mm)	Image size	Megapixel (MP)	Central band and bandwidth (nm)	Radiometric resolution (BIT)
DJI Phantom 4 multispectral	Multispectral	5.74	1,600 × 1,300	2.08	Red: 650 ± 16 Green: 560 ± 16 Blue: 450 ± 16 RedEdge: 730 ± 16 NIR: 840 ± 26	16
	RGB	5.74	1,600 × 1,300	20	n.a.	8

Table 2. Characteristics of the performed flights. GSD means Ground Sample Distance.

	Autumn			Spring		
	A1	A2	A3	A1	A2	A3
Average height (m)	77	76	89	64	62	87
Average GSD multispectral (cm)	3.95	3.91	4.55	3.15	3.01	4.52
Area (km^2)	0.114	0.098	0.122	0.176	0.088	0.044
Number of images	460	573	246	674	494	271

We conducted the flights with nadiral camera orientation with an overlap of 80%. The Autumn flight resulted in 1,279 frames, while the Spring flights produced 1,439 frames (Table 2).

We processed the collected data using the Agisoft Metashape Software (Agisoft Metashape 2021), following a standard structure from motion (SfM) approach capable of handling multiband information. Subsequently, RGB and multispectral datasets underwent separate analyses through a conventional SfM workflow (Figure 3).

We calibrated the multispectral datasets using the embedded irradiance sensor in the DJI Phantom. The ground points in the RGB point cloud were automatically classified utilizing an algorithm integrated into the processing software, and a digital terrain model (DTM) was generated through interpolation.

We georeferenced the 3D models directly in the WGS84-UTM 32 coordinate system via direct photogrammetry (Chiabrando, Lingua, and Piras 2013), thanks to the drone's built-in dual-frequency GNSS receiver. We validated the UAS GNSS accuracy by means of reference points measured through GNSS in the network real-time kinematic (NRTK) technique, achieving accuracies of 3 cm for the *Up* component and 1.5 cm for the *East* and *North* components, with fixed-phase ambiguity at all points.

Furthermore, we geolocated 973 tree and shrub species (Table 3) in the field by referencing their centers. This database was fundamental in training and validating the canopy classification, as elucidated in the subsequent section.

2.3. Species classification

We initiated object-based image analysis (OBIA), which consists of a semantic segmentation process where each object corresponds to an individual plant. Subsequently, we applied a machine-learning algorithm to identify and classify the plant species (Figure 3). The primary steps in this methodology included: i) image segmentation; ii) extraction of features and preparation of data; iii) creation of training and testing datasets; iv) classification of the datasets; v) selection of features; and vi) validation and evaluation of the model's reproducibility.

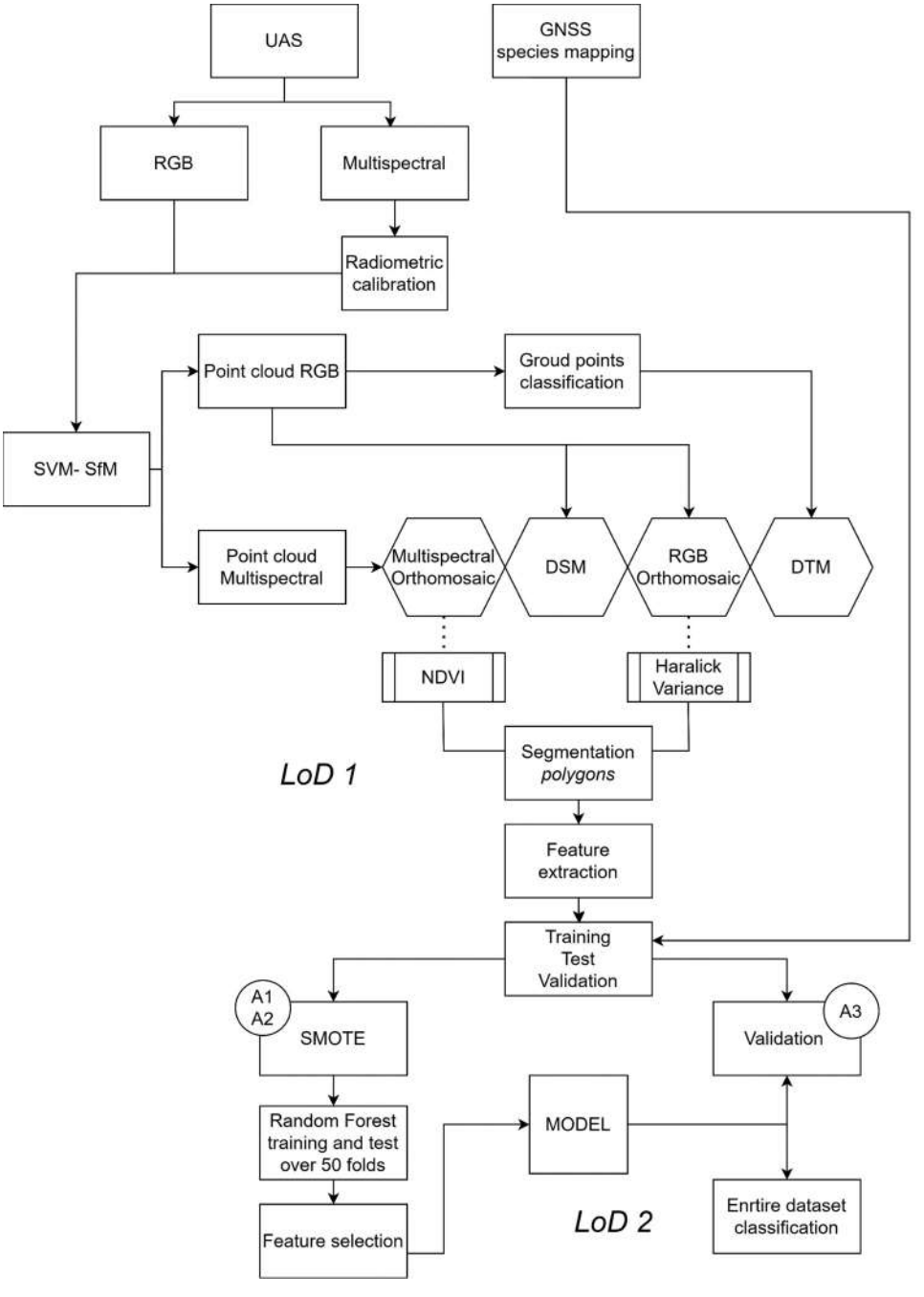

Figure 3. Workflow of the two-level-of-detail OBIA UHR classification model.

2.4. Individual plant detection

In the existing literature, numerous algorithms designed for the segmentation of individual tree crowns, commonly known as individual tree detection (ITD) algorithms, have been extensively employed in forestry (Dalponte et al. 2018; Latella, Sola, and Camporeale 2021).

Table 3. Classes of the classification and number of the mapped samples.

Species	ID	Number of samples		Species	ID	Number of samples	
Debris (service class)	Det	101	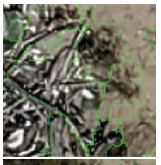	*Daphne Gnidium* L.	Dg	101	
Sand (service class)	Sab	91		*Pancratium maritimum* L.	Pm	72	
Ammophila arenaria L.	Aa	174		*Eryngium maritimum* L.	Em	49	
Juniperus oxycedrus macrocarpa L.	Jo	145		*Pinus Pinaster* Ait.	Pp	49	
Helichrysum stoechas L.	Hes	122		*Yucca gloriosa* L.	Yg	43	
Euphorbia paralias L.	Ep	114		*Achillea maritima (L.) Ehrend. & Y. P. Guo*	Am	25	
Dittrichia viscosa (L.) Greuter	Dv	18	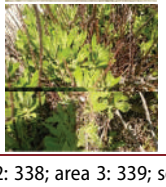	*Echinophora spinosa L.*	Es	25	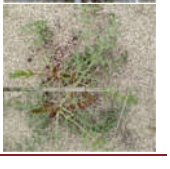

Mapped samples in area 1: 260; area 2: 338; area 3: 339; service classes not included.

While these solutions are typically tailored for 2.5D LiDAR-sourced datasets and high-resolution optical data, some examples of single-individual segmentation for shrub species also exist. However, these segmentation algorithms often rely on identifying treetops, proving to be less effective for canopies with a globular shape, such as broadleaf trees and shrubs. In light of these considerations, we opted for a texture-based system, as previously implemented in (Belcore et al. 2020). Specifically, we computed texture measures based on the Haralick co-occurrence grey level matrix (CGLM), with mean and variance values calculated over a 5×5-pixel neighborhood on the green band (Haralick, Shanmugam, and Dinstein 1973).

We conducted the segmentation process through *eCognition Developer (Trimble)*, a commercial development platform for segmentation and object-oriented classification. We identified vegetated areas with NDVI from the Spring set to 0.12 and Haralick Mean lower than 2.8 m to generate a vegetation mask. Also, we established a textural threshold through a manual iterative process to balance the exclusion of too little grass and data noise without disregarding the low photosynthetic part of the plants (Figure 1) and photosynthetic algae on large woody debris near the seashore. Using the multiresolution algorithm, we merged adjacent pixels into objects, with scaling, shape, and compactness parameters set to 39, 0.7, and 0.5, respectively. Finally, we excluded segments from the vegetation class if they had an average value of Haralick textural variance greater than 1.7 or an average DN value of Haralick textural mean less than 1.0. The minimum mapping unit is 10 cm^2.

2.5. Feature extraction

We generated new classification variables by combining and applying statistical measures to the input data. This process, referred to as feature extraction, enhances the model with more meaningful information than the original variables alone, especially in complex classification models (Horning et al. 2020). We produced a total of 47 features, including seven spectral indices per epoch, eight texture measures based on the co-occurrence grey level matrix (Haralick) per epoch, one elevation-based feature, and sixteen radiometric bands (Table 4).

2.6. Data preparation and classification algorithm

We implemented the classification algorithm in *Python*, utilizing the *Pandas*, *NumPy*, and *Sklearn* libraries. After exporting segments from *eCognition* as shapefiles, each containing the average digital number (DN) of associated features for the segmented objects, we assigned species information based on GNSS locations gathered from the field. Preparing the data for analysis involved removing null values and invalid geometries, with feature scaling based on minimum and maximum values.

To give meaning to all the segments of LoD1, we introduced two service classes: debris and sand. The final classification dataset comprised 1,045 samples. We applied oversampling to address the dataset's imbalance since the largest classes had around 100 samples and the smallest only 18. Specifically, we employed the borderline synthetic minority oversampling technique for classification (SMOTE) (Chawla et al. 2002), interpolating and reducing the nearest neighbors of the smallest class. We considered four neighboring samples for each class and only two for the smaller class, applying the borderline SMOTE algorithm solely to the training dataset, resulting in a final dataset of 2,436 samples.

We adopted a random forest classifier (Breiman 2001) with 2,000 trees, using the Gini criterion for node splitting since the literature confirmed random forest methods to be reliable in UHR classification (Bhatt and Maclean 2023; N. Zhang et al. 2023). We cross-validated the decision tree model on areas 1 and 2 using k-fold validation ($k = 50$), computing average overall accuracy, the standard deviation for each fold, and the F1 score for each class. We applied a threshold of 0.75 times the average impurity to exclude features with higher uncertainty or impurity

Table 4. Input features in the proposed classification model.

	Features	Formula and notes	Reference
Spectral indices	Enhanced Vegetation Index (EVI)	It indicates vegetation in areas with high leaf area index. $2.5 \times \frac{NIR-Red}{(NIR+(6.0*Red)-(7.5*Blue)+1.0)}$	(A. A. Huete et al. 2002)
	MRENDVI	$\frac{(RedEdge-NIR)}{RedEdge+NIR-(2*Blue)}$	(Datt 1999)
	MCARI	$((RedEdge - Red) - 0.2*(RedEdge - Green))*\left(\frac{RedEdge}{Red}\right)$ It indicates the relative abundance of chlorophyll. It is illumination and non-photosynthetic materials invariant. (Daughtry et al. 2000)	(Daughtry et al. 2000)
	Soil-Adjusted Vegetation Index (SAVI)	$\frac{(NIR-Red)}{(NIR+Red+0.5)}$	(A. R. Huete 1988)
	Soil Redness Index (RI)	$\frac{Red^2}{Green^3}$	(Bannari et al. 1995)
	Normalized Difference Vegetation Index (NDVI)	It indicates the vegetated regions and the plant vigour. $\frac{(NIR-Red)}{(NIR+Red)}$	(Kriegler et al. 1969)
	Normalized Difference Water Index NIR, (NDWI)	It highlights open water bodies. It is insensitive to built-up land, vegetation, and soil. $\frac{(Green-NIR)}{(Green+NIR)}$ (McFeeters 2013)	(McFeeters 2013)
GLCM textural measures	Contr	Contrast; it measures the local contrast of an image.	(Haralick, Shanmugam, and Dinstein 1973)
	Entr	Entropy; it measures the local entropy in an image.	
	Asm	Angular Second Moment; it measures the number of repeated pairs.	
	Corr	Correlation; it measures the correlation between pairs of pixels.	
	Idm (homogeneity)	Inverse Difference Moment; it measures the homogeneity.	
	Mean	Mean.	
	Diss	Dissimilarity.	
	StdDev	Standard deviation.	
DEM	NDSM	Crown height elevation model: NDSM = DSM – DTM	

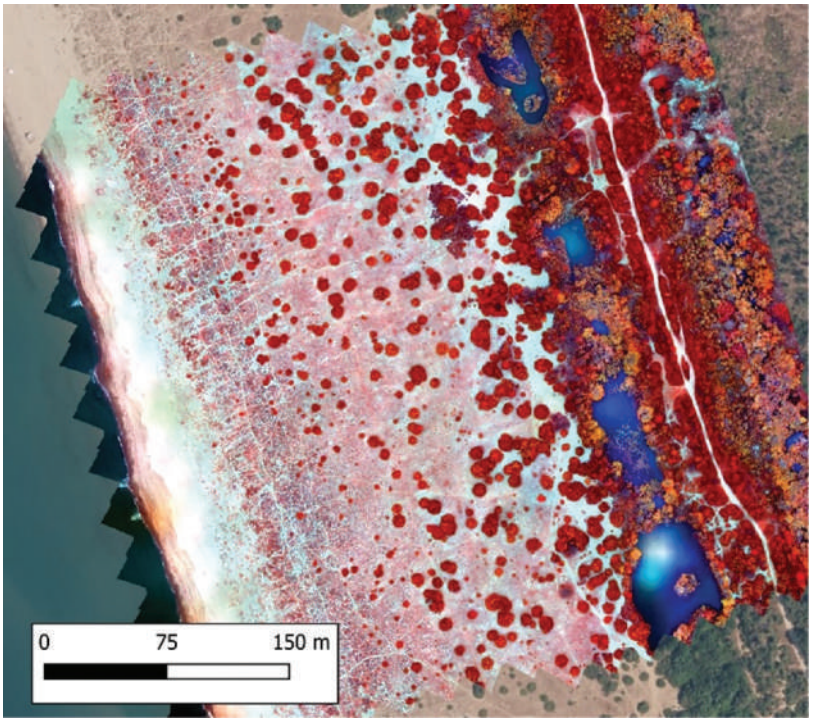

Figure 4. False-colour (NGR) visualization of area 1 orthomosaic, *Spring* data acquisition. Basemap from Google satellite.

from the model (importance analysis). Subsequently, we assessed the model's generalization capability by applying it to study area 3. Additionally, we trained, ran, and evaluated the model while excluding textural information from the Haralick co-occurrence grey level matrix to determine its impact on classification performance.

3. Results

3.1. Photogrammetric processing

The photogrammetric process yielded two orthomosaics (RGB and multispectral), a digital surface model (DSM), and a digital terrain model (DTM) for each epoch. The multispectral orthomosaics consistently exhibit a slightly lower spatial resolution than the RGB ones, owing to the varying sensor resolutions (Table 1). Specifically, the spectral resolution of the multispectral orthomosaic in the Autumn epoch is 4 cm, while in the Spring epoch, it is 3 cm. The RGB orthomosaics have a ground sample distance (GSD) of 3 cm for Autumn and 2 cm for Spring. The digital elevation models were uniformly generated at a 4 cm resolution. All products were georeferenced in the cartographic reference system EPSG 32,632. Figure 4 provides an example of the resulting orthomosaics, showcasing small-scale dune vegetation in the initial coastal strip, succeeded by larger junipers and pines, leading to a shift in tree species, primarily maritime pines, in areas characterized by water stagnation.

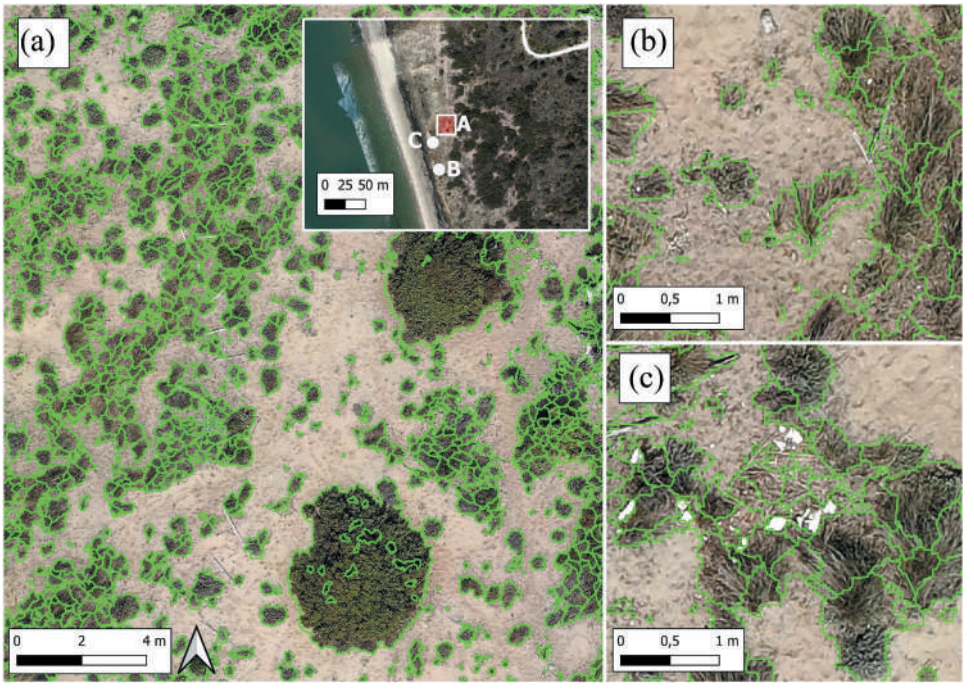

Figure 5. (a) Example of overall segmentation at the first level of detail (LoD1) and detail of segmentation in areas covered by (b) *Ammophila arenaria* only and (c) *Ammophila arenaria* with plastic debris.

3.2. Individual plant detection and classification

The segmentation process generated 7,092 individual segments, each representing a single plant (see Figure 5 for an example). The output of the first level of detail (LoD1) ultra high-resolution (UHR) model included the individual plant segmentations exported as a shapefile in EPSG:32632.

The average overall accuracy, computed as the arithmetic mean over 50 folds, is 0.76, with a standard deviation of 0.09 (Table 5). After removing the least important features, the same metric calculated on the folds yields an identical overall accuracy, with a standard deviation of 0.08 (Table 6). F1 values for each class were computed for each fold, both with and without feature selection. The accuracy analysis was also conducted on the dataset without textural information (Table 7).

The model trained in areas 1 and 2 was tested in area 3 to evaluate its generalization capacity, attaining an overall accuracy of 0.62 and satisfactory F1 scores for each class (Table 8). A visual representation of the results is provided in Figure 6.

4. Discussion

Numerous investigations underscored the significance of monitoring and mapping coastal ecosystems by applying high-resolution data (Agrillo et al. 2022; Cruz et al. 2023; Fabbri et al. 2021; Suo, McGovern, and Gilmer 2019; Yousefi Lalimi et al. 2017).

Table 5. Summary of validation results.

Cross-validation over 50 folds	Debris (service class)	Sand (service class)	Ammophila arenaria L.	Juniperus oxycedrus macrocarpa L.	Helichrysum stoechas L.	Euphorbia paralias L.	Daphne Gnidium L.	Pancratium maritimum L.	Eryngium maritimum L.	Pinus Pinaster Ait.	Yucca gloriosa L.	Achillea maritima (L.) Ehrend. & Y. P. Guo	Echinophora spinosa L.	Dittrichia viscosa (L.) Greuter
	Det	Sab	Aa	Jo	Hes	Ep	Dg	Pm	Em	Pp	Yg	Am	Es	Dv
Minimum precison	0.39	0.53	0.82	0.82	0.73	0.70	0.65	0.79	o.65	0.61	o.44	0.37	o.42	0.15
Minimum precision F.S.	0.38	0.55	0.87	0.83	0.68	0.69	0.63	0.78	0.57	0.65	0.44	0.34	0.39	0.21
Minimum recall	0.4	0.58	0.94	0.86	0.81	0.66	0.66	0.76	0.72	0.66	0.46	0.38	0.42	0.16
Minimum recall F.S	0.44	0.58	0.90	0.86	0.76	0.65	0.64	0.78	0.70	0.74	0.48	0.36	0.40	0.22
Minimum F1	0.51	0.41	0.85	0.81	0.72	0.67	0.63	0.76	0.62	0.65	0.42	0.37	0.41	0.15
Minimum F1 F.S.	0.53	0.46	0.86	0.83	0.72	0.67	0.63	0.76	0.59	0.70	0.42	0.37	0.39	0.17
Mean overall accuracy					0.764				**Standard deviation**				0.090	
Mean overall accuracy F.S.					0.763				**Standard deviation F.S.**				0.080	

F.S. means feature selection.

Table 6. Importance values of the input features. Only the features marked with (*) were included in the final model.

Epoch	Feature	Importance	Epoch	Feature	Importance
I	NDWI*	0.044	I	GLCM_Entr*	0.023
II	NDSM*	0.043	II	GLCM_Contr*	0.022
I	EVI*	0.042	I	blue_multisp*	0.021
I	NDVI*	0.039	I	red_multisp*	0.019
I	SAVI*	0.038	I	green_multisp*	0.019
I	RI*	0.037	I	GLCM_Asm*	0.019
I	Red_RGB*	0.036	II	NDWI*	0.016
II	blue_multisp*	0.036	II	EVI	0.014
II	Red_RGB*	0.033	I	NIR	0.014
II	RI*	0.032	II	GLCM_Homog	0.014
I	MCARI*	0.030	I	RedEdge	0.012
II	red_multisp*	0.030	II	GLCM_StdDev	0.011
II	NIR*	0.030	II	MRENDVI	0.009
II	Blue_RGB*	0.028	I	MRENDVI	0.009
II	Green_RGB*	0.028	I	GLCM_Mean	0.005
II	MCARI*	0.027	II	GLCM_Entr	0.004
I	GLCM_Diss*	0.027	II	GLCM_Asm	0.003
II	green_multisp*	0.026	I	GLCM_Homog	0.003
II	SAVI*	0.026	II	GLCM_Diss	0.003
II	NDVI*	0.025	I	GLCM_StdDev	0.003
I	Blue_RGB*	0.024	II	GLCM_Mean	0.002
I	GLCM_Corr*	0.024	I	GLCM_Contr	0.002
I	Green_RGB*	0.023	II	GLCM_Corr	0.002
II	RedEdge*	0.023			

Notably, most of these studies employed spatial resolutions in the order of centimeters. Yet, although this resolution would allow operating at the individual plant level, these works generally focused on collective or group-level analyses. However, it is worth noting that in-depth monitoring can facilitate biogeomorphological studies (i.e. research on mutual land-vegetation co-adjustments) and land management since plants have a pivotal role in dune formation and consolidation. Thus, this work aimed to provide a methodology to gain precise information about the location and attributes of individual species and plants to support the investigation of the coastal dune ecosystem and its spatial and temporal evolution.

We started by observing that each segmented pixel group represents an individual plant in an environment characterized by low plant density. Consequently, we decided to adopt an object-based image analysis (OBIA) classification approach, which indeed resulted in being robust (Figure 5(a)). Only slight inaccuracies were found in this classification, mainly related to the false detection of individuals within the larger plants (Junipers) and caused by low NDVI values (dry branches) cut out by the first level of detail (LoD1) NDVI threshold. Among the analyzed species, the segmentation of *Ammophila arenaria* presented remarkable complexity since it engenders the formation of continuous land cover (*Ammophila arenaria* prairies). Nonetheless, we leveraged some physical characteristics of these plants to enhance segmentation (Figure 5(b)), like their dry center with high DN values (high reflectance) and the low DN response of their leaves, which are often shaded. Indeed, despite not being verifiable, we assumed that the dry centrer of the plant and the texture oriented in a single direction might positively impact the segmentation. Overall, the classification exhibits favorable outcomes, demonstrating the efficacy of the model, but also the challenge of addressing areas featuring plastic debris or sparse vegetation where segmentation accuracy diminishes (Figure 5(c)).

Table 7. Validation results of the dataset without the textural information.

Cross-validation over 50 folds without texture	Debris (service class)	Sand (service class)	Ammophila arenaria L.	Juniperus oxycedrus macrocarpa L.	Helichrysum stoechas L.	Euphorbia paralias L.	Daphne Gnidium L.	Pancratium maritimum L.	Eryngium maritimum L.	Pinus Pinaster Ait.	Yucca gloriosa L.	Achillea maritima (L.) Ehrend. & Y. P. Guo	Echinophora spinosa L.	Dittrichia viscosa (L.) Greuter
	Det	Sab	Aa	Jo	Hes	Ep	Dg	Pm	Em	Pp	Yg	Am	Es	Dv
Minimum precison	0.31	0.36	0.89	0.81	0.73	0.64	0.65	0.78	0.56	0.59	0.36	0.32	0.29	0.2
Minimum recall	0.36	0.4	0.9	0.81	0.74	0.61	0.64	0.8	0.62	0.72	0.4	0.34	0.36	0.22
Minimum F1	0.33	0.37	0.87	0.79	0.7	0.6	0.61	0.77	0.58	0.63	0.37	0.33	0.21	0.21
Mean overall accuracy					0.726				**Standard deviation**				0.10	

Table 8. Replicability results.

Replicability test on area 3	Debris (service class)	Sand (service class)	Ammophila arenaria L.	Juniperus oxycedrus macrocarpa L.	Helichrysum stoechas L.	Euphorbia paralias L.	Daphne Gnidium L.	Pancratium maritimum L.	Eryngium maritimum L.	Pinus Pinaster Ait.	Yucca gloriosa L.	Achillea maritima (L.) Ehrend. & Y. P. Guo	Echinophora spinosa L.	Dittrichia viscosa (L.) Greuter
	Det	Sab	Aa	Jo	Hes	Ep	Dg	Pm	Em	Pp	Yg	Am	Es	Dv
Precision	0.65	0.70	0.66	0.52	0.42	0.22	0.57	1.00	0.20	0.76	0.60	0.00	0.00	0.86
Recall	0.84	0.85	0.90	0.68	0.26	0.17	0.63	0.44	0.04	0.97	0.50	0.00	0.00	0.33
F1-score	0.73	0.77	0.76	0.59	0.32	0.19	0.59	0.61	0.07	0.85	0.55	0.00	0.00	0.48
Overall accuracy										0.621				

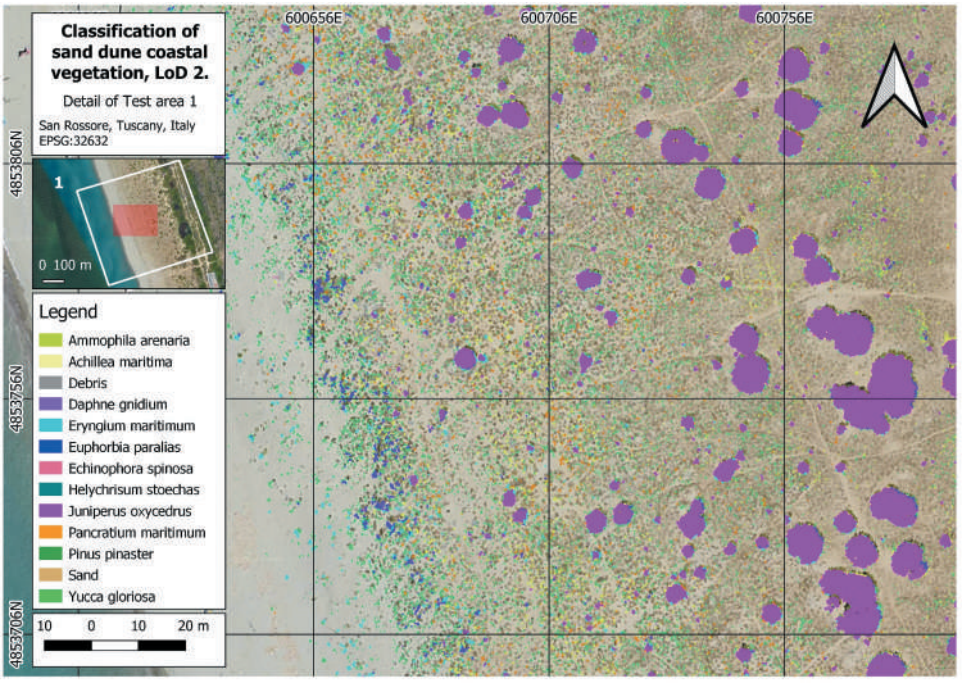

Figure 6. Example of the classification results from area 1.

Looking at the classes individually (Table 5), the lowest F1 scores are found for *Yucca gloriosa* (0.42), *Achillea maritima* (0.37), *Echinophora spinosa* (0.39) and *Dittrichia viscosa* (0.17). The poor performance of these species can be attributed to both the model and the limited number of samples available (only 25), except for *Yucca gloriosa*. Also, the morphological characteristics and behavior of these species might have contributed to low accuracy. Indeed, *Achillea maritima* and *Echinophora spinosa* are generally small-sized, with very thin stems and leaves that are difficult to identify, even in UHR images. Furthermore, *Dittrichia viscosa* and *Yucca gloriosa* grow in the shade of other species like *Pinus pinaster* and *Juniperus oxycedrus macrocarpa* that might hide them during the segmentation.

Counterintuitively, the sand class shows a low F1 score, although this class was expected to be easily identified given the abundance of sand samples and the presence of sand in homonymous segments. Sand and debris were defined as service classes because small segments with high NDVI values were present in the segmentation, not being masked in LoD1. These small high-NDVI segments represent those small-sized herbaceous patches alternating with sandy areas. The attempts to eliminate these segments using elevation data (i.e. a normalized digital surface model, NDSM) information resulted in the loss of the lower parts of many species, thus making this way unpracticable. Similarly, debris areas are characterized by alternating vegetation, sometimes algae and woody debris, which are impossible to separate even with texture measurements. The resulting low performance of the sand class is likely due to the variability of the selected samples. Since service classes significantly lowered the overall model performance during

our tests, we recommend not using them, and our future works will address the issue of improving the LoD1 while avoiding service classes.

Since we initially hypothesized that textural information could improve classification, we assessed the same model without it. As a result, we found a decrease in classification performance, underscoring the relevance of texture in UHR vegetation classification, as suggested by (Kupidura 2019; Shen and Sarris 2008). The texture-based segmentation was able to distinguish samples belonging to different species but with similar spectral responses (Table 6). Indeed, we remark that there is pronounced heterogeneity in the pixel response for the same object in the coastal dune environment but little spectral variability among different classes (i.e. species). For example, *Euphorbia paralias* and *Daphne Gnidium* classes are characterized by a similar spectral response and internal variability. Consequently, it would have been challenging to separate these two species using only reflectance and radiometric indices if two specimens were found close. Therefore, the texture-based segmentation proved helpful in their discretization by considering the alternation and spatial distribution of pixels within the samples.

An examination of feature importance highlighted that, despite the improvement related to the inclusion of texture in segmentation, radiometric and height information holds greater significance in classification. The NDSM, commonly employed in 2.5D segmentations, exhibits less influence on herbaceous and shrubby vegetation due to challenges in identifying treetops as abrupt changes in Digital Number (DN) spatial distribution. Segmentation posed increased difficulty for grasses, primarily *Ammophila arenaria*, forming continuous and dense patches, making on-site differentiation challenging.

While there are fewer instances of single-individual segmentation for shrub species for direct comparison, existing studies typically focus on vegetation distribution based on area coverage rather than individual plant counts. In our study, the relatively low vegetation density in dune environments enabled semantic segmentation based on texture data. However, smaller species were inevitably not accurately segmented and often overlooked, exemplified by *Medicago littoralis*, which was excluded from classification due to its excessively small size and challenging identification.

A comprehensive evaluation of the model's replicability (Table 8), revealed satisfactory generalization, evidenced by an overall accuracy of 0.62. In Area 3, misclassifications were observed for Achillea maritima and Echinophora spinosa, which resulted in a reduced F1 score for *Eryngium maritimum*. This discrepancy is attributed to the lower orthomosaic resolution in Area 3 (4.5 cm), which is a consequence of a higher flight altitude. Contrary to expectations, *Dittrichia viscosa* and sand were better identified, but both *Dittrichia viscosa* and *Helichrysum stoechas* exhibited low recall compared to precision, indicating the presence of false negatives.

This work presented a straightforward application of the proposed model and underscored the feasibility of ultra-high-resolution (UHR) vegetation classification, particularly when associating radiometric and texture information with precise field surveys. Nevertheless, it highlighted persistent challenges, such as determining the appropriate ground sample distance (GSD) for identifying habitat-characterizing species. Notably, our classification did not encompass all species but focused on larger and more prevalent ones, contributing to the resulting classification error.

Given the widespread availability of deep learning models, it could have been possible to apply a deep learning model for the case study in this work. However, we chose a more traditional random forest approach because it requires a smaller training dataset. A simplified and generalized rule states that a deep learning model needs a large training dataset and no feature extraction, while classical machine learning models can exist with small training datasets but many features. Indeed, a significant limitation in natural environments is obtaining extensive labeled datasets. Considering the vastness of the areas and the challenges in data collection, the field-measured labels are not sufficient to construct a robust model. Additionally, due to the similarity among species, distinguishing between different species in the orthomosaics proved to be challenging, even for the human eye. Overall, considering the low accuracy of sand and debris, we recommend further work to address sand, debris, and vegetation detection at LoD1. In this work, we demonstrate that UHR is invaluable when complementing field measurements in coastal dune environments. Indeed, field measurements in sandy and coastal areas often encounter challenges such as limited accessibility, long distances, and the need for repeated, time-consuming efforts to gather representative datasets. Additionally, interpolating punctual field data to cover larger scales may compromise representativeness in heterogeneous coastal environments. UAS UHR surveys, coupled with the proposed classification method, address these challenges by providing detailed, multi-temporal information over a continuous spatial domain, minimizing in-field work.

To conclude, this approach generates substantial data for supporting diverse scientific research endeavors, ranging from characterizing vegetation patterns (Sperandii et al. 2019) to exploring the interplay between sand transport and plant dynamics (Latella et al. 2021; Yousefi Lalimi et al. 2017) and monitoring coastal restoration (Fabbri et al. 2021). Furthermore, the data generated supports biogeomorphological modeling by offering initial vegetation and topographical scenarios or serving as validation data. When finely tuned, these models offer unparalleled opportunities for comprehensive analyses of coastal areas, particularly in facilitating the upscaling of UAS data to high-resolution (0.5 m) optical satellite data for broader applications.

5. Conclusions

This work explored the potential of using ultra-high-resolution multispectral data for mapping vegetation of coastal dune ecosystems. For this purpose, we classified several plant species in three study areas in the San Rossore Regional Park (Italy). We worked on orthomosaics with a ground sample distance (GSD) of approximately 3–5 cm and set up a classification model with two hierarchical levels of detail (LoD) based on random forest classification and object-based image analysis (OBIA). With our application, we demonstrated the reliability of our model and paved the way for future research on model generalization and downsampling, which could be achieved by applying the presented model to similar datasets and including very high-resolution satellite imagery. Also, feature engineering could improve our model by investigating other texture measures, such as fractals. To sum up, the present work set a first step to leverage LoD-OBIA approaches to support coastal dune monitoring and other studies, from analyzing vegetation patterns to phytosociology and biogeomorphological modeling at a fine scale.

Acknowledgements

The Migliarino, San Rossore, Massaciuccoli Regional Park Authority has endorsed this study.

Disclosure statement

No potential conflict of interest was reported by the author(s).

Funding

ML was supported by the EO4EU (AI-augmented ecosystem for Earth Observation data accessibility with Extended reality User Interfaces forService and data exploitation) project, funded by the EU's Horizon Europe Research and Innovation Programme under Grant Agreement No. 101060784.

ORCID

E. Belcore http://orcid.org/0000-0002-3592-9384
M. Latella http://orcid.org/0000-0003-3678-6992
M. Piras http://orcid.org/0000-0001-8000-2388
C. Camporeale http://orcid.org/0000-0002-7311-6018

Data availability statement

The data that support the findings of this study are available from the corresponding author, ML, upon reasonable request.

References

Acosta, A., C. Blasi, and A. Stanisci. 2009. "Spatial Connectivity and Boundary Patterns in Coastal Dune Vegetation in the Circeo National Park, Central Italy." *Journal of Vegetation Science* 11 (febbraio): 149–154. https://doi.org/10.2307/3236787.

Agisoft Metashape. 2021. Accessed febbraio 12, 2021. https://www.agisoft.com/.

Agrillo, E., F. Filipponi, R. Salvati, A. Pezzarossa, and L. Casella. 2022. "Modeling Approach for Coastal Dune Habitat Detection on Coastal Ecosystems Combining Very High-Resolution UAV Imagery and Field Survey." *Remote Sensing in Ecology and Conservation* 9 (2): 251–267. https://doi.org/10.1002/rse2.308.

Ahmed, O. S., A. Shemrock, D. Chabot, C. Dillon, G. Williams, R. Wasson, and S. E. Franklin. 2017. "Hierarchical Land Cover and Vegetation Classification Using Multispectral Data Acquired from an Unmanned Aerial Vehicle." *International Journal of Remote Sensing* 38 (8–10): 2037–2052. https://doi.org/10.1080/01431161.2017.1294781.

Babaeian, E., S. Paheding, N. Siddique, V. K. Devabhaktuni, and M. Tuller. 2021. "Estimation of Root Zone Soil Moisture from Ground and Remotely Sensed Soil Information with Multisensor Data Fusion and Automated Machine Learning." *Remote Sensing of Environment* 260 (luglio): 112434. https://doi.org/10.1016/j.rse.2021.112434.

Bannari, A., D. Morin, F. Bonn, and A. R. Huete. 1995. "A Review of Vegetation Indices." *Remote Sensing Reviews* 13 (1–2): 95–120. https://doi.org/10.1080/02757259509532298.

Barducci, A., D. Guzzi, P. Marcoionni, and I. Pippi. 2009. "Aerospace Wetland Monitoring by Hyperspectral Imaging Sensors: A Case Study in the Coastal Zone of San Rossore Natural Park." *Journal of Environmental Management* 90 (7): 2278–2286. https://doi.org/10.1016/j.jenvman.2007.06.033.

Barducci, A., D. Guzzi, P. Marcoionni, I. Pippi, and S. Raddi. 2007. *PROBA Contribution to Wetland Monitoring in the Coastal Zone of San Rossore Natural Park*. Montreux, Switzerland: European Space Agency, (Special Publication) ESA SP.

Belcore, E., M. Latella, M. Disney, and K. Anderson. 2022. "Riparian Ecosystems Mapping at Fine Scale: A Density Approach Based on Multi-Temporal UAV Photogrammetric Point Clouds." *Remote Sensing in Ecology and Conservation* 8 (5): 644–655. https://doi.org/10.1002/rse2.267.

Belcore, E., M. Piras, and A. Pezzoli. 2022. "Land Cover Classification from Very High-Resolution UAS Data for Flood Risk Mapping." *Sensors* 22 (15): 5622. https://doi.org/10.3390/s22155622.

Belcore, E., M. Pittarello, A. Maria Lingua, and M. Lonati. 2021. "Mapping Riparian Habitats of Natura 2000 Network (91E0*, 3240) at Individual Tree Level Using UAV Multi-Temporal and Multi-Spectral Data." *Remote Sensing* 13 (9): 1756. https://doi.org/10.3390/rs13091756.

Belcore, E., A. Wawrzaszek, E. Wozniak, N. Grasso, and M. Piras. 2020. "Individual Tree Detection from UAV Imagery Using Hölder Exponent." *Remote Sensing* 12 (15): 2407. https://doi.org/10.3390/rs12152407.

Belloni, V., M. Di Rita, D. Fugazza, G. Traversa, K. Hanson, G. Diolaiuti, and M. Crespi. 2023. "High-Resolution High-Accuracy Orthophoto Map and Digital Surface Model of Forni Glacier Tongue (Central Italian Alps) from UAV Photogrammetry." *Journal of Maps* 19 (1): 2217508. https://doi.org/10.1080/17445647.2023.2217508.

Bertacchi, A. 2017. "Dune Habitats of the Migliarino – San Rossore – Massaciuccoli Regional Park (Tuscany – Italy)." *Journal of Maps* 13 (2): 322–331. https://doi.org/10.1080/17445647.2017.1302365.

Bertoni, D., F. Alquini, M. Bini, D. Ciccarelli, R. Giaccari, A. Pozzebon, A. Ribolini, and G. Sarti. 2014. "A Technical Solution to Assess Multiple data Collection on Beach Dunes: the Pilot site of Migliarino San Rossore Regional park (Tuscany, Italy)." *Atti Della Società Toscana Di Scienze Naturali Residente in Pisa Memorie Serie A*, 116:5–12. https://doi.org/10.2424/ASTSN.M.2014.10.

Bhatt, P., and A. L. Maclean. 2023. "Comparison of High-Resolution NAIP and Unmanned Aerial Vehicle (UAV) Imagery for Natural Vegetation Communities Classification Using Machine Learning Approaches." *GIScience & Remote Sensing* 60 (1): 2177448. https://doi.org/10.1080/15481603.2023.2177448.

Breiman, L. 2001. "Random Forests." *Machine Learning* 45 (1): 5–32. https://doi.org/10.1023/A:1010933404324.

Calantropio, A., F. Chiabrando, G. Sammartano, A. Spanò, and L. Teppati Losè. 2018. "Uav Strategies Validation and Remote Sensing data for Damage Assessment in Post-Disaster Scenarios." In *ISPRS - International Archives of the Photogrammetry, Remote Sensing and Spatial Information Sciences*, 121–128. Vol. XLII-3-W4. Copernicus GmbH. https://doi.org/10.5194/isprs-archives-XLII-3-W4-121-2018.

Campos-Taberner, M., F. Javier García-Haro, B. Martínez, S. Sánchez-Ruiz, Á. Moreno-Martínez, G. Camps-Valls, and M. Amparo Gilabert. 2023. "Land Use Classification Over Smallholding Areas in the European Common Agricultural Policy Framework." *ISPRS Journal of Photogrammetry & Remote Sensing* 197 (marzo): 320–334. https://doi.org/10.1016/j.isprsjprs.2023.02.005.

Carboni, M., M. Laura Carranza, and A. Acosta. 2009. "Assessing Conservation Status on Coastal Dunes: A Multiscale Approach." *Landscape and Urban Planning* 91 (1): 17–25. https://doi.org/10.1016/j.landurbplan.2008.11.004.

Chawla, N. V., K. W. Bowyer, L. O. Hall, and W. P. Kegelmeyer. 2002. "SMOTE: Synthetic Minority Over-Sampling Technique." *The Journal of Artificial Intelligence Research* 16 (giugno): 321–357. https://doi.org/10.1613/jair.953.

Chiabrando, F., A. Lingua, and M. Piras. 2013. "Direct Photogrammetry Using Uav: Tests and First Results." In *ISPRS - International Archives of the Photogrammetry, Remote Sensing and Spatial Information Sciences*, 81–86. Vol. XL-1-W2. Copernicus GmbH. https://doi.org/10.5194/isprsarchives-XL-1-W2-81-2013.

Ciccarelli, D. 2014. "Mediterranean Coastal Sand Dune Vegetation: Influence of Natural and Anthropogenic Factors." *Environmental Management* 54 (2): 194–204. https://doi.org/10.1007/s00267-014-0290-2.

Ciccarelli, D., F. Garbari, and G. Bedini. 2009. "Plant Functional Types in Tuscan Coastal Dunes." *Flora Mediterranea 1120-4052* 19 (gennaio): 199–206.

Cipriani, L. E., A. Perfetti, E. Pranzini, and G. Vitale. 2010. *Azioni di tutela delle dune costiere del Parco Regionale Migliarino San Rossore Massaciuccoli (Toscana settentrionale)*, 165–179. Vol. 17. Firenze, Italy: Studi costieri.

Cortesi, I., A. Masiero, G. Tucci, and K. Topouzelis. 2022. "Uav-Based River Plastic Detection with a Multispectral Camera." *International Archives of the Photogrammetry, Remote Sensing and Spatial Information Sciences* XLIII-B3-2022:855–861. https://doi.org/10.5194/isprs-archives-XLIII-B3-2022-855-2022.

Cruz, C., J. O'Connell, K. McGuinness, J. R. Martin, P. M. Perrin, and J. Connolly. 2023. "Assessing the Effectiveness of UAV Data for Accurate Coastal Dune Habitat Mapping." *European Journal of Remote Sensing* 56 (1): 2191870. https://doi.org/10.1080/22797254.2023.2191870.

Dalponte, M., L. Frizzera, H. Ole Ørka, T. Gobakken, E. Næsset, and D. Gianelle. 2018. "Predicting Stem Diameters and Aboveground Biomass of Individual Trees Using Remote Sensing Data." *Ecological Indicators* 85 (febbraio): 367–376. https://doi.org/10.1016/j.ecolind.2017.10.066.

Datt, B. 1999. "A New Reflectance Index for Remote Sensing of Chlorophyll Content in Higher Plants: Tests Using Eucalyptus Leaves." *Journal of Plant Physiology* 154 (1): 30–36. https://doi.org/10.1016/S0176-1617(99)80314-9.

Daughtry, C. S. T., C. L. Walthall, M. S. Kim, E. Brown de Colstoun, and J. E. McMurtrey. 2000. "Estimating Corn Leaf Chlorophyll Concentration from Leaf and Canopy Reflectance." *Remote Sensing of Environment* 74 (2): 229–239. https://doi.org/10.1016/S0034-4257(00)00113-9.

Diez, Y., S. Kentsch, M. Fukuda, M. Larry Lopez Caceres, K. Moritake, and M. Cabezas. 2021. "Deep Learning in Forestry Using Uav-Acquired Rgb Data: A Practical Review." *Remote Sensing* 13 (14): 2837.

Di Gregorio, A., and Food and Agriculture Organization of the Unitedations. 2005. *Land Cover Classification System: Classification Concepts and User Manual: LCCS*. Roma, Italy: Food & Agriculture Org.

Fabbri, S., E. Grottoli, C. Armaroli, and P. Ciavola. 2021. "Using High-Spatial Resolution UAV-Derived Data to Evaluate Vegetation and Geomorphological Changes on a Dune Field Involved in a Restoration Endeavour." *Remote Sensing* 13 (10): 1987. https://doi.org/10.3390/rs13101987.

Fanini, L., G. Maria Marchetti, F. Scapini, and O. Defeo. 2007. "Abundance and Orientation Responses of the Sandhopper Talitrus Saltator to Beach Nourishment and Groynes Building at San Rossore Natural Park, Tuscany, Italy." *Marine Biology* 152 (5): 1169–1179. https://doi.org/10.1007/s00227-007-0764-3.

Fawcett, D., J. Bennie, and K. Anderson. 2021. "Monitoring Spring Phenology of Individual Tree Crowns Using Drone-Acquired NDVI Data." *Remote Sensing in Ecology and Conservation* 7 (2): 227–244. https://doi.org/10.1002/rse2.184.

Gellini, R., F. Pantani, P. Grossoni, F. Bussotti, E. Barbolani, and C. Rinallo. 1983. "Survey of the Deterioration of the Coastal Vegetation in the Park of San Rossore in Central Italy." *European Journal of Forest Pathology* 13 (5–6): 296–304. https://doi.org/10.1111/j.1439-0329.1983.tb00130.x.

Gromny, E., J. Haarpaintner, S. Aleksandrowicz, M. Jenerowicz, E. Wozniak, L. Pesquer, and Z. Pawlak. 2022. *Land Cover Change Analysis Around the Mtendeli Refugee Camp in Tanzania*. https://doi.org/10.13140/RG.2.2.31837.08169.

Haralick, R. M., K. Shanmugam, and I. Dinstein. 1973. "Textural Features for Image Classification." *IEEE Transactions on Systems, Man, and Cybernetics* SMC-3 (6): 610–621. https://doi.org/10.1109/TSMC.1973.4309314.

Herold, M., J. S. Latham, A. Di Gregorio, and C. C. Schmullius. 2006. "Evolving Standards in Land Cover Characterization." *Journal of Land Use Science* 1 (2–4): 157–168. https://doi.org/10.1080/17474230601079316.

Horning, N. 2020. "Land Cover Mapping with Ultra-High-Resolution Aerial Imagery." *Remote Sensing in Ecology and Conservation* 6 (4): 429–430. https://doi.org/10.1002/rse2.189.

Horning, N., E. Fleishman, P. J. Ersts, F. A. Fogarty, M. Wohlfeil Zillig, N. Pettorelli, and M. Disney. 2020. "Mapping of Land Cover with Open-Source Software and Ultra-High-Resolution Imagery

Acquired with Unmanned Aerial Vehicles." *Remote Sensing in Ecology and Conservation* 6 (4): 487–497. https://doi.org/10.1002/rse2.144.

Huete, A. R. 1988. "Soil-Adjusted Vegetation Index (SAVI)." *Remote Sensing of Environment* 25 (3): 295–309. https://doi.org/10.1016/0034-4257(88)90106-X.

Huete, A., K. Didan, T. Miura, E. P. Rodriguez, X. Gao, and L. G. Ferreira. 2002. "Overview of the Radiometric and Biophysical Performance of the MODIS Vegetation Indices." *Remote Sensing of Environment* 83 (1): 195–213. https://doi.org/10.1016/S0034-4257(02)00096-2.

Ioli, F., L. Pinto, D. Passoni, V. Nova, and M. Detert. 2020. "Evaluation of Airborne Image Velocimetry Approaches Using Low-Cost Uavs in Riverine Environments." In *The International Archives of the Photogrammetry, Remote Sensing and Spatial Information Sciences*, 597–604. Vol. XLIII-B2-2020. Copernicus GmbH. https://doi.org/10.5194/isprs-archives-XLIII-B2-2020-597-2020.

Kalantar, B., S. Bin Mansor, M. Ibrahim Sameen, B. Pradhan, and H. Z. M. Shafri. 2017. "Drone-Based Land-Cover Mapping Using a Fuzzy Unordered Rule Induction Algorithm Integrated into Object-Based Image Analysis." *International Journal of Remote Sensing* 38 (8–10): 2535–2556. https://doi.org/10.1080/01431161.2016.1277043.

Kattenborn, T., J. Eichel, S. Wiser, L. Burrows, F. E. Fassnacht, S. Schmidtlein, N. Horning, and N. Clerici. 2020. "Convolutional Neural Networks Accurately Predict Cover Fractions of Plant Species and Communities in Unmanned Aerial Vehicle Imagery." *Remote Sensing in Ecology and Conservation* 6 (4): 472–486. https://doi.org/10.1002/rse2.146.

Kriegler, F. J., W. A. Malila, R. F. Nalepka, and W. Richardson. 1969. "Preprocessing Transformations and Their Effects on Multispectral Recognition." Proceedings of the Sixth International Symposium on Remote Sensing of Environment, October 13–16. Vol. II, 97–131.

Kupidura, P. 2019. "The Comparison of Different Methods of Texture Analysis for Their Efficacy for Land Use Classification in Satellite Imagery." *Remote Sensing* 11 (10): 1233. https://doi.org/10.3390/rs11101233.

Kuras, A., M. Brell, J. Rizzi, and I. Burud. 2021. "Hyperspectral and Lidar Data Applied to the Urban Land Cover Machine Learning and Neural-Network-Based Classification: A Review." *Remote Sensing* 13 (17): 3393. https://doi.org/10.3390/rs13173393.

Kutiel, P. 2001. "Conservation and Management of the Mediterranean Coastal Sand Dunes in Israel." *Journal of Coastal Conservation* 7 (2): 183–192. https://doi.org/10.1007/BF02742480.

Laporte-Fauret, Q., B. Lubac, B. Castelle, R. Michalet, V. Marieu, L. Bombrun, P. Launeau, M. Giraud, C. Normandin, and D. Rosebery. 2020. "Classification of Atlantic Coastal Sand Dune Vegetation Using in Situ, UAV, and Airborne Hyperspectral Data." *Remote Sensing* 12 (14): 2222. https://doi.org/10.3390/rs12142222.

Latella, M., A. Luijendijk, A. M. Moreno-Rodenas, and C. Camporeale. 2021. "Satellite Image Processing for the Coarse-Scale Investigation of Sandy Coastal Areas." *Remote Sensing* 13 (22): 4613. https://doi.org/10.3390/rs13224613.

Latella, M., F. Sola, and C. Camporeale. 2021. "A Density-Based Algorithm for the Detection of Individual Trees from LiDAR Data." *Remote Sensing* 13 (2): 322. https://doi.org/10.3390/rs13020322.

Lou, P., T. Wu, J. Chen, B. Fu, X. Zhu, J. Chen, X. Wu, et al. 2023. "Recognition of Thaw Slumps Based on Machine Learning and UAVs: A Case Study in the Qilian Mountains, Northeastern Qinghai-Tibet Plateau." *International Journal of Applied Earth Observation and Geoinformation* 116 (febbraio): 103163. https://doi.org/10.1016/j.jag.2022.103163.

Maun, M. A. 2020. *The Biology of Coastal Sand Dunes*. Oxford: Oxford University Press.

McFeeters, S. K. 2013. "Using the Normalized Difference Water Index (NDWI) within a Geographic Information System to Detect Swimming Pools for Mosquito Abatement: A Practical Approach." *Remote Sensing* 5 (7): 3544–3561. https://doi.org/10.3390/rs5073544.

Melville, B., A. Fisher, and A. Lucieer. 2019. "Ultra-High Spatial Resolution Fractional Vegetation Cover from Unmanned Aerial Multispectral Imagery." *International Journal of Applied Earth Observation and Geoinformation* 78 (giugno): 14–24. https://doi.org/10.1016/j.jag.2019.01.013.

Michez, A., H. Piégay, J. Lisein, H. Claessens, and P. Lejeune. 2016. "Classification of Riparian Forest Species and Health Condition Using Multi-Temporal and Hyperspatial Imagery from Unmanned

Aerial System." *Environmental Monitoring and Assessment* 188 (3): 146. https://doi.org/10.1007/s10661-015-4996-2.

Mo, A., M. D'Antraccoli, G. Bedini, and D. Ciccarelli. 2021. "The Role of Plants in the Face of Marine Litter Invasion: A Case Study in an Italian Protected Area." *Marine Pollution Bulletin* 169 (agosto): 112544. https://doi.org/10.1016/j.marpolbul.2021.112544.

Natesan, S., C. Armenakis, and U. Vepakomma. 2020. "Individual Tree Species Identification Using Dense Convolutional Network (DenseNet) on Multitemporal RGB Images from UAV." *Journal of Unmanned Vehicle Systems* 8 (4): 310–333. https://doi.org/10.1139/juvs-2020-0014.

Park, G., K. Park, B. Song, and H. Lee. 2022. "Analyzing Impact of Types of UAV-Derived Images on the Object-Based Classification of Land Cover in an Urban Area." *Drones* 6 (3): 71. https://doi.org/10.3390/drones6030071.

Patrucco, G., F. Giulio Tonolo, G. Sammartano, and A. Spanò. 2022. "Sfm-Based 3D Reconstruction of Heritage Assets Using Uav Thermal Images." *International Archives of the Photogrammetry, Remote Sensing and Spatial Information Sciences* XLIII-B1-2022:399–406. https://doi.org/10.5194/isprs-archives-XLIII-B1-2022-399-2022.

Piégay, H., F. Arnaud, B. Belletti, M. Bertrand, S. Bizzi, P. Carbonneau, S. Dufour, F. Liébault, V. Ruiz-Villanueva, and L. Slater. 2020. "Remotely Sensed Rivers in the Anthropocene: State of the Art and Prospects." *Earth Surface Processes and Landforms* 45 (1): 157–188. https://doi.org/10.1002/esp.4787.

Prošek, J., and P. Šímová. 2019. "UAV for Mapping Shrubland Vegetation: Does Fusion of Spectral and Vertical Information Derived from a Single Sensor Increase the Classification Accuracy?" *International Journal of Applied Earth Observation and Geoinformation* 75 (marzo): 151–162. https://doi.org/10.1016/j.jag.2018.10.009.

Räsänen, A., S. Juutinen, E.-S. Tuittila, M. Aurela, T. Virtanen, and D. Rocchini. 2019. "Comparing Ultra-High Spatial Resolution Remote-Sensing Methods in Mapping Peatland Vegetation." *Journal of Vegetation Science* 30 (5): 1016–1026. https://doi.org/10.1111/jvs.12769.

Ritchie, W. 1972. "The Evolution of Coastal Sand Dunes." *Scottish Geographical Magazine* 88 (1): 19–35. https://doi.org/10.1080/00369227208736205.

Sankey, J. B., T. T. Sankey, J. Li, S. Ravi, G. Wang, J. Caster, and A. Kasprak. 2021. "Quantifying Plant-Soil-Nutrient Dynamics in Rangelands: Fusion of UAV Hyperspectral-LiDAR, UAV Multispectral-Photogrammetry, and Ground-Based LiDAR-Digital Photography in a Shrub-Encroached Desert Grassland." *Remote Sensing of Environment* 253 (febbraio): 112223. https://doi.org/10.1016/j.rse.2020.112223.

Schiefer, F., T. Kattenborn, A. Frick, J. Frey, P. Schall, B. Koch, and S. Schmidtlein. 2020. "Mapping Forest Tree Species in High Resolution UAV-Based RGB-Imagery by Means of Convolutional Neural Networks." *Isprs Journal of Photogrammetry & Remote Sensing* 170 (dicembre): 205–215. https://doi.org/10.1016/j.isprsjprs.2020.10.015.

Scopetani, C., D. Chelazzi, T. Martellini, J. Pellinen, A. Ugolini, C. Sarti, and A. Cincinelli. 2021. "Occurrence and Characterization of Microplastic and Mesoplastic Pollution in the Migliarino San Rossore, Massaciuccoli Nature Park (Italy)." *Marine Pollution Bulletin* 171 (ottobre): 112712. https://doi.org/10.1016/j.marpolbul.2021.112712.

Shen, G., and A. Sarris. 2008. "Application of Texture Analysis in Land Cover Classification of High Resolution Image." *2008 Fifth International Conference on Fuzzy Systems and Knowledge Discovery*, 513–517. Jinan Shandong, China: IEEE. https://doi.org/10.1109/FSKD.2008.241.

Shi, Y., T. Wang, A. K. Skidmore, and M. Heurich. 2020. "Improving LiDAR-Based Tree Species Mapping in Central European Mixed Forests Using Multi-Temporal Digital Aerial Colour-Infrared Photographs." *International Journal of Applied Earth Observation and Geoinformation* 84 (febbraio): 101970. https://doi.org/10.1016/j.jag.2019.101970.

Sothe, C., M. Dalponte, C. M. de Almeida, M. Benedito Schimalski, C. Luciane Lima, V. Liesenberg, G. Takahashi Miyoshi, and A. Maria Garcia Tommaselli. 2019. "Tree Species Classification in a Highly Diverse Subtropical Forest Integrating UAV-Based Photogrammetric Point Cloud and Hyperspectral Data." *Remote Sensing* 11 (11): 1338. https://doi.org/10.3390/rs11111338.

Sperandii, M. G., M. Bazzichetto, A. Teresa Rosario Acosta, V. Barták, and M. Malavasi. 2019. "Multiple Drivers of Plant Diversity in Coastal Dunes: A Mediterranean Experience." *Science of the Total Environment* 652 (febbraio): 1435–1444. https://doi.org/10.1016/j.scitotenv.2018.10.299.

Suo, C., E. McGovern, and A. Gilmer. 2019. "Coastal Dune Vegetation Mapping Using a Multispectral Sensor Mounted on an UAS." *Remote Sensing* 11 (15): 1814. https://doi.org/10.3390/rs11151814.

Takahashi Miyoshi, G., N. N. Imai, A. M. Garcia Tommaselli, M. V. Antunes de Moraes, and E. Honkavaara. 2020. "Evaluation of Hyperspectral Multitemporal Information to Improve Tree Species Identification in the Highly Diverse Atlantic Forest." *Remote Sensing* 12 (2): 244. https://doi.org/10.3390/rs12020244.

Townshend, J. G. 1992. "Land Cover." *International Journal of Remote Sensing* 13 (6–7): 1319–1328. https://doi.org/10.1080/01431169208904193.

Trevisiol, F., A. Lambertini, F. Franci, and E. Mandanici. 2022. "An Object-Oriented Approach to the Classification of Roofing Materials Using Very High-Resolution Satellite Stereo-Pairs." *Remote Sensing* 14 (4): 849. https://doi.org/10.3390/rs14040849.

Turner, B. L., F. L. Eric, and A. Reenberg. 2007. "The Emergence of Land Change Science for Global Environmental Change and Sustainability." *Proceedings of the National Academy of Sciences* 104 (52): 20666–20671. https://doi.org/10.1073/pnas.0704119104.

Verburg, P. H., P. Alexander, T. Evans, N. R. Magliocca, Z. Malek, M. Da Rounsevell, and J. Van Vliet. 2019. "Beyond Land Cover Change: Towards a New Generation of Land Use Models." *Current Opinion in Environmental Sustainability* 38 (giugno): 77–85. https://doi.org/10.1016/j.cosust.2019.05.002.

Wawrzyniak, V., H. Piégay, P. Allemand, L. Vaudor, and P. Grandjean. 2013. "Prediction of Water Temperature Heterogeneity of Braided Rivers Using Very High Resolution Thermal Infrared (TIR) Images." *International Journal of Remote Sensing* 34 (13): 4812–4831. https://doi.org/10.1080/01431161.2013.782113.

Woodget, A. S., R. Austrums, I. P. Maddock, and E. Habit. 2017. "Drones and Digital Photogrammetry: From Classifications to Continuums for Monitoring River Habitat and Hydromorphology." *WIREs Water* 4 (4): e1222. https://doi.org/10.1002/wat2.1222.

Wulder, M. A., N. C. Coops, D. P. Roy, J. C. White, and T. Hermosilla. 2018. "Land Cover 2.0." *International Journal of Remote Sensing* 39 (12): 4254–4284. https://doi.org/10.1080/01431161.2018.1452075.

Wyard, C., B. Beaumont, T. Grippa, and E. Hallot. 2022. "UAV-Based Landfill Land Cover Mapping: Optimizing Data Acquisition and Open-Source Processing Protocols." *Drones* 6 (5): 123. https://doi.org/10.3390/drones6050123.

Yousefi Lalimi, F., S. Silvestri, L. J. Moore, and M. Marani. 2017. "Coupled Topographic and Vegetation Patterns in Coastal Dunes: Remote Sensing Observations and Ecomorphodynamic Implications: Ecogeomorphic Patterns in Coastal Dunes." *Journal of Geophysical Research: Biogeosciences* 122 (1): 119–130. https://doi.org/10.1002/2016JG003540.

Zhang, N., X. Chai, N. Li, J. Zhang, and T. Sun. 2023. "Applicability of UAV-Based Optical Imagery and Classification Algorithms for Detecting Pine Wilt Disease at Different Infection Stages." *GIScience & Remote Sensing* 60 (1): 2170479. https://doi.org/10.1080/15481603.2023.2170479.

Zhang, X., G. Chen, W. Wang, Q. Wang, and F. Dai. 2017. "Object-Based Land-Cover Supervised Classification for Very-High-Resolution UAV Images Using Stacked Denoising Autoencoders." *IEEE Journal of Selected Topics in Applied Earth Observations & Remote Sensing* 10 (7): 3373–3385. https://doi.org/10.1109/JSTARS.2017.2672736.

Zollini, S., M. Alicandro, D. Dominici, R. Quaresima, and M. Giallonardo. 2020. "UAV Photogrammetry for Concrete Bridge Inspection Using Object-Based Image Analysis (OBIA)." *Remote Sensing* 12 (19): 3180. https://doi.org/10.3390/rs12193180.